Autonomic Cardiovascular Control Following Transient Arousal From Sleep: A Time-Varying Closed-Loop Model

Anna Blasi, Javier Antonio Jo, Edwin Valladares, Ricardo Juarez, Ahmet Baydur, and Michael C. K. Khoo*, *Member, IEEE*

***Abstract*—Recent studies suggest that exposure to repetitive episodes of hypoxia and transient arousal can lead to increased risk for cardiovascular disease in patients with obstructive sleep apnea syndrome (OSAS). To obtain an improved understanding of and to quantitatively characterize the autonomic effects of arousal from sleep, a time-varying closed-loop model was used to determine the interrelationships among respiration, heart rate and blood pressure in 8 normal adults. A recursive least squares algorithm was used in combination with the Laguerre expansion technique to estimate the time-varying impulse responses of the 4 model components. We found that during arousal: 1) respiratory-cardiac coupling gain increases in nonrapid-eye movement (NREM) but not in REM sleep; 2) in both NREM and REM sleep, baroreflex gain shows an initial increase, but this is followed by a more sustained decrease below pre-arousal baseline levels, allowing sympathetic tone to be elevated over a relatively long duration; 3) the gains of other model components show increases with arousal that are consistent with the increased sympathetic modulation of systemic vascular resistance and contractility of the heart. These findings establish a normative database against which further measurements of cardiovascular arousal responses in OSAS may be compared.**

***Index Terms*—Adaptive filtering, baroreflex, blood pressure variability, heart rate variability, respiratory sinus arrhythmia, system identification.**

I. Introduction

It is now well-accepted that patients with sleep-related breathing disorders, the most common being obstructive sleep apnea syndrome (OSAS), are at increased risk of developing hypertension and other cardiovascular disease [1]. Abnormally high sympathetic tone and impaired parasympathetic activity are believed to be primary causal factors that lead to these adverse cardiovascular consequences of OSAS [2]. It has been hypothesized that these alterations in autonomic function, in turn, result from chronic exposure to the episodes of hypoxia and arousal from sleep associated with repetitive upper airway obstruction [1].

While much research has focused on determining the effects of intermittent hypoxia on cardiovascular function [3], [4], much less attention has been paid to investigating the autonomic cardiovascular effects of arousal from sleep. The arousals associated with OSAS are largely transient, lasting 3 s or more, and generally are not associated with any overall change in sleep stage [5]. In human nonrapid-eye movement (NREM) sleep, acoustically-induced arousals have been found to increase muscle sympathetic nerve activity, systolic and diastolic blood pressure, heart rate and respiratory tidal volume within the first few seconds of the arousal [6]–[8]. In a recent study, we found that low-frequency (LF) heart rate variability and blood pressure variability remained at elevated levels up to 40 s following the start of arousal [9]. This suggested that the repetitive occurrence of such arousals might lead to a cumulative increase in sympathoexcitation. One important limitation of this and other univariate analyses of heart rate or blood pressure is that they do not provide clear insights into the behavior of the underlying autonomic mechanisms during the transient state changes due to the closed-loop nature of these mechanisms. As well, previous studies only examined the cardiovascular responses to arousal during nonrapid eye movement (NREM) sleep; REM sleep was not considered.

In the present study, we have adopted a different strategy for analyzing these changes. We have modeled the interrelationships among respiration, heart rate and blood pressure as a nonstationary closed-loop system, and applied system identification techniques to estimate the time-varying model parameters during both NREM and REM arousals. The analysis was carried out in the time domain, since it was necessary to impose causality constraints in order to computationally delineate the feedback from feedforward components of the closed-loop model. By applying the model-based analysis to data obtained from healthy subjects during sleep, we were able to establish a normative database against which further work on cardiovascular arousal responses in OSAS may be compared.

II. Methods

A. Subjects and Signals

The electrocardiogram (ECG), continuous blood pressure and changes in respiratory volume (VT) were recorded in a set of

Manuscript received November 4, 2004; revised April 10, 2005. This work was supported by the National Institutes of Health (NIH) under Grant EB-001978 and Grant HL-076375. *Asterisk indicates corresponding author.*

A. Blasi was with the Department of Biomedical Engineering, University of Southern California, Los Angeles, CA 90089 USA. She is now with the Department of Medical Physics and Bioengineering, University College London, London WC1E 6BT U.K.

J. A. Jo is with the Biophotonics Research & Technology group at Cedars-Sinai Medical Center, Los Angeles, CA 90048 USA.

E. Valladares is with the Department of Biomedical Engineering, University of Southern California, Los Angeles, CA 90089 USA.

R. Juarez and A. Baydur are with the Department of Medicine, University of Southern California, Los Angeles, CA 90089 USA.

*M. C. K. Khoo is with the Department of Biomedical Engineering, OHE-500, University of Southern California, Los Angeles, CA 90089–1451 USA.

Digital Object Identifier 10.1109/TBME.2005.859789

experiments conducted overnight on a group of 8 normal subjects (41.80 ± 5.98 yrs of age and 26.32 ± 1.74 kg/m2 BMI, in mean ± SE) at the General Clinical Research Center of the Los Angeles County/USC Medical Center. Written informed consent was obtained from each subject prior to participation in the study. Each recording was 4-min long, beginning 1 min before the application of a binaural acoustic stimulus. After each trial with a successful arousal, the subject was allowed to sleep for a few minutes before starting a new experiment. Due to the instrumentation, some subjects had difficulty sleeping and did not reach REM stage, while in others the number of experiments performed in this sleep stage was too small to be taken in account for the analysis. Thus, comparisons involving REM sleep include data from only 5 subjects throughout this work.

Each subject was connected via nasal mask to a bilevel positive airway pressure (BiPAP) device (Model S/T-D 30, Respironics Inc., Murraysville, PA) that delivered a minimal pressure of 2–3 cm H2O throughout the study. The purpose of applying the minimal pressure was to overcome the resistance of the breathing circuit and also to minimize the effects of changes in upper airway resistance on respiratory airflow during sleep and arousal.

A chin strap was applied to prevent leakage of airflow through the mouth. Pressure within the mask, and inspiratory and expiratory airflow were acquired by recording the patient output signals obtained from the Detachable Control Panel (DCP 30, Respironics Inc., Murraysville, PA) available for use with the BiPAP system. Continuous arterial blood pressure was monitored noninvasively by means of an arterial tonometer (Model 7000, Colin Medical Instruments, San Antonio, TX), along with a single-lead electrocardiogram (BMA-831 bioamplifier, CWE Inc., Ardmore, PA). The other standard polysomnographic variables were monitored using the Easy II Sleep System (Cadwell Laboratories, Kennewick, WA). These included O2 saturation, 3 electroencephalogram derivations (C4/A1, C3/A2 and O1/A2), chin electromyogram, left and right electrooculogram, and leg movements. The acoustic stimulus intensity employed in each experimental trial ranged from 55 to 90 dB, and was adjusted so that EEG arousals [5] were elicited without producing outright awakening. The frequency of the applied auditory stimulus was 1 kHz, lasting for up to 0.5 s. The recorded data were digitized at 200 Hz per channel.

B. Data Analysis

1) Pre-Processing: Pre-processing of the data consisted of extracting the R-R intervals (RRIs) and systolic blood pressure (SBP) on a beat-to-beat basis from the ECG and continuous blood pressure signals and downsampling these to 2 Hz. using the Berger algorithm [10]. After preprocessing, we used the first minute of each recording (pre-arousal data) to obtain preliminary estimates of the number of model parameters (number of Laguerre coefficients) and α, the parameter that controls the rate of decay of the impulse response function (see the Appendix).

2) The Model: To characterize the interrelationships among respiration, RRI and SBP, we assumed a closed-loop model, similar in structure to that previously published by our group [11], [12] and others [13], [14]. In this model, fluctuations of RRI are influenced by SBP via the arterial baroreflex (labeled "ABR")

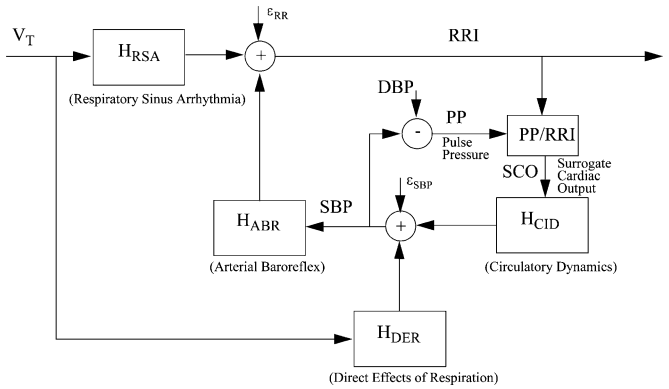

Fig. 1. Model of the cardiovascular control system modified from [11] and [12]. Glossary of symbols: VT = respiratory volume, RRI = R-R interval, SBP = systolic blood pressure, DBP = diastolic blood pressure, PP = pulse pressure, SCO = surrogate cardiac output, $\varepsilon_{\mathrm{RR}}$ = unknown stochastic influences on RRI, $\varepsilon_{\mathrm{RR}}$ = unknown stochastic influences on SBP, $\mathrm{H_{RSA}}$ = transfer function representing respiratory-cardiac coupling, $\mathrm{H_{ABR}}$ = transfer function representing baroreflex dynamics, $\mathrm{H_{CID}}$ = transfer function representing circulatory dynamics, $\mathrm{H_{DER}}$ = transfer function representing the direct influence of respiratory-related intrathoracic pressure changes on blood pressure.

mechanism and respiration via direct respiratory-cardiac coupling (labeled "RSA," since this mechanism is primarily responsible for the respiratory sinus arrhythmia). Fluctuations in SBP are assumed to be influenced by changes in intrathoracic pressure that result from respiration (labeled "DER," for "direct effects of respiration"), and by variations in cardiac output governed by the Frank-Starling and Windkessel runoff effects (labeled "CID," for circulatory dynamics) [13]. We defined a new variable, the "surrogate cardiac output" (SCO), in the following way: at beat n, $\mathrm{SCO}(n) = \mathrm{PP}(n)/\mathrm{RRI}(n)$, where $\mathrm{PP}(n) = \mathrm{SBP}(n) - \mathrm{DBP}(n)$ (DBP being diastolic blood pressure). SCO was then used as the input to the CID transfer function and SBP as considered the "output" of this component (Fig. 1). Thus, the estimated CID impulse response was expected to be largely representative of the combined impedance properties of the heart and systemic vasculature. The DER impulse response represents the dynamics of the transmission between respiratory fluctuations and fluctuations in SBP; this could include the mechanical transmission of intrathoracic pressure to arterial blood pressure as well as the direct effect of respiration on stroke volume via respiratory-driven sympathetic modulation of heart contractility [15].

The equations that represent these relations are as follows:

$$\begin{aligned}\Delta\mathrm{RRI}(t) = &\sum_{i=0}^{M-1} h_{\mathrm{RSA}}(t,i)\cdot\Delta V_T(t-i-\tau_{\mathrm{RSA}}) \\ &+ \sum_{i=0}^{M-1} h_{\mathrm{ABR}}(t,i)\cdot\Delta SBP(t-i-\tau_{\mathrm{SBP}}) \\ &+ \varepsilon_{RR}(t) \qquad (1)\end{aligned}$$

$$\begin{aligned}\Delta\mathrm{SBP}(t) = &\sum_{i=0}^{M-1} h_{\mathrm{CID}}(t,i)\cdot\Delta\mathrm{SCO}(t-i-\tau_{\mathrm{CID}}) \\ &+ \sum_{i=0}^{M-1} h_{\mathrm{MER}}(t,i)\cdot\Delta V_T(t-i) \\ &+ \varepsilon_{\mathrm{SBP}}(t) \qquad (2)\end{aligned}$$

In the above equations, $h_{\mathrm{RSA}}(t,i)$, $h_{\mathrm{ABR}}(t,i)$, $h_{\mathrm{CID}}(t,i)$, and $h_{\mathrm{DER}}(t,i)$ represent the time-varying impulse responses of the corresponding model components, while $\tau_{\mathrm{RSA}}, \tau_{\mathrm{ABR}}, \tau_{\mathrm{CID}}$, and τ_{DER} represent the corresponding time-delays. $\varepsilon_{\mathrm{RRI}}(t)$ and $\varepsilon_{\mathrm{SBP}}(t)$ represent the respective discrepancies (errors) between the model predictions and the measurements of RRI and SBP, representing those aspects of the data that are not explained by the model.

3) Model Analysis: A detailed account of the method for estimating the time-varying impulse responses from the data is given in the Appendix. Briefly, each time-varying impulse response in (1) and (2) was expressed as a Laguerre expansion according to the method proposed by Marmarelis [16]; however, in this case, the expansion coefficients were allowed to be time-varying. The recursive least squares (RLS) algorithm was employed for adaptive estimation of these coefficients [17]. One of the advantages of projecting the signals on the Laguerre basis is that the method provides a significant reduction of the number of parameters that need to be estimated; as well, the estimated impulse responses are smoothed. On the other hand, a limitation is that using specific combinations of Laguerre functions inevitably implies some constraint on the possible shapes of the estimated impulse responses, thus leading to a certain degree of bias in the estimation. Another advantage of the Laguerre expansion technique is the ability to expand the model to incorporate nonlinearity in the dynamics [16]. This, however, is obtained at the cost of a significant increase in parametrization and consequent reduction in statistical reliability of the parameter estimates, particularly when the model is allowed to be time-varying. Given the short data segments that were available for analysis, we chose to adopt the most parsimonious model possible and, thus, excluded nonlinear contributions.

4) Impulse Response Descriptors: Compact descriptors were used to facilitate the characterization of the time-varying impulse responses, thereby allowing statistical tests to be applied. These included: the *impulse response magnitude*, *dynamic gain* and *characteristic time* [18]. The first two descriptors convey information about the gain of the component in question. The last descriptor, *characteristic time*, provides information about the latency of the impulse response. The *impulse response magnitude* was measured as the difference between the first significant maximum and minimum of the impulse response. The *dynamic gain* was computed as the average gain of the frequency response between 0.04 and 0.5 Hz, which covers the range of frequencies of interest. *Characteristic time* was defined as follows:

$$\text{Characteristic time} = \frac{\sum_{t=0}^{M-1} t\,|h(t)|}{\sum_{t=0}^{M-1} |h(t)|} \tag{3}$$

C. Tests on Simulated Data

The aforementioned algorithm was first tested on simulated "data" (y) generated from a dual-input model (inputs: x and u). One branch of the model contained an impulse response resembling that of the ABR component, whereas the other branch contained an impulse response similar to that of the RSA component. These impulse responses were assumed to remain unchanged until a given time when they were abruptly altered in magnitude: the gain of the ABR component was abruptly increased (Fig. 2, top panel), whereas the gain of the RSA component was abruptly decreased (Fig. 2, bottom panel). This model was subjected to input excitation using real respiration and SBP waveforms selected from our database. The output of the model contained the sum of the responses of the two model components and Gaussian white noise (representing output measurement noise); the coefficient of variation (noise/signal) was 10%. The estimation algorithm was applied to determine whether it could accurately and reliably track the abrupt changes in these impulse responses. The top and bottom panels of Fig. 3 display examples of the time-varying impulse responses estimated for the ABR and RSA components, respectively. The abrupt change in model impulse responses occurred at $t = 120$ samples (highlighted by the appearance of the rectangular frame in Fig. 3). Based on the application of our analysis to several realizations of these simulations, we found that the model was able to track these abrupt changes in the impulse responses of both input branches following an adjustment period of between 20 and 40 samples (or, in terms of absolute time, between 10 and 20 s).

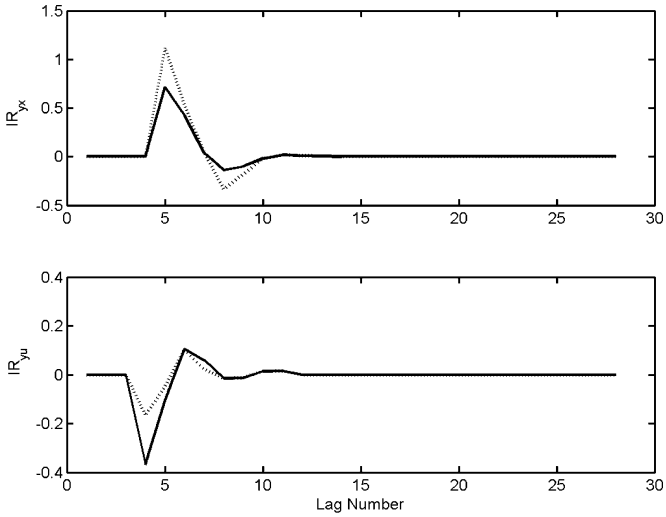

Fig. 2. Model impulse responses from transfer functions between inputs x and output y ($\mathrm{IR_{yx}}$), and input u and output y ($\mathrm{IR_{yu}}$), used in simulation tests. Solid tracings: impulse responses before simulated arousal; broken tracings: impulse responses after simulated arousal.

D. Statistical Analysis

The number of experiments where an arousal was scored ranged between 3 and 17 per sleep stage per patient. Every trial was analyzed using the aforementioned method. However, for each subject, the median value at each time-point of the impulse response was computed, and the time-course of these median values was taken to be representative of the estimated impulse response of that individual. Subsequently, the compact descriptors were derived from the median impulse response time-course. The statistical analysis performed on each compact descriptor consisted of first testing whether or not arousal modified the value of the parameter in time versus its averaged pre-arousal value using one-way repeated-measures analysis

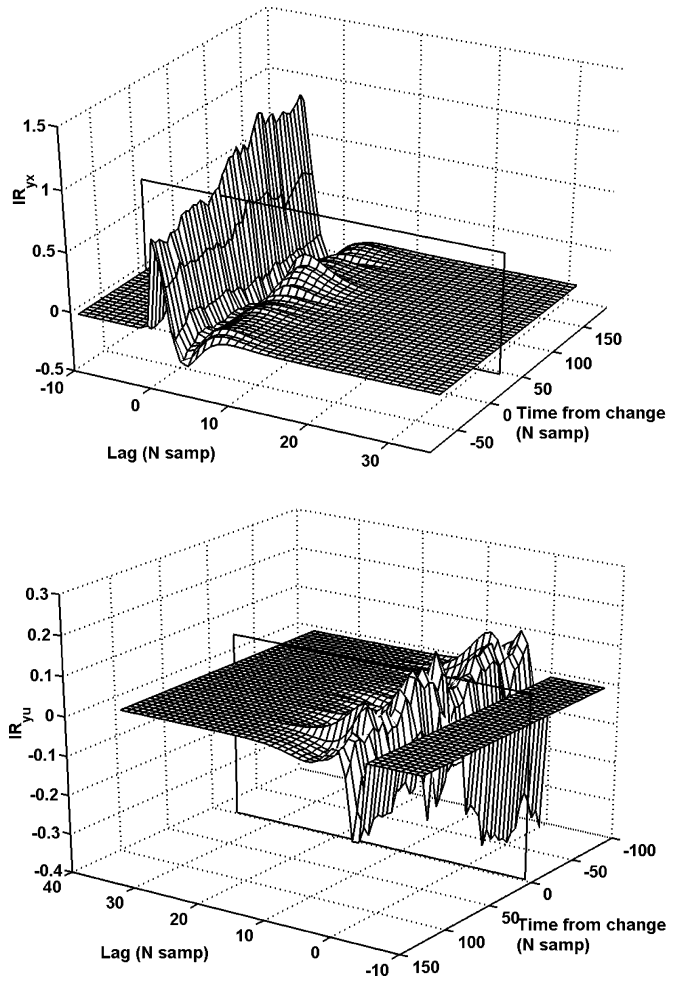

Fig. 3. Time-varying ABR (top panel) and RSA (bottom panel) impulse responses estimated from simulated "data". Transparent rectangular plane denotes time of abrupt change in model impulse responses.

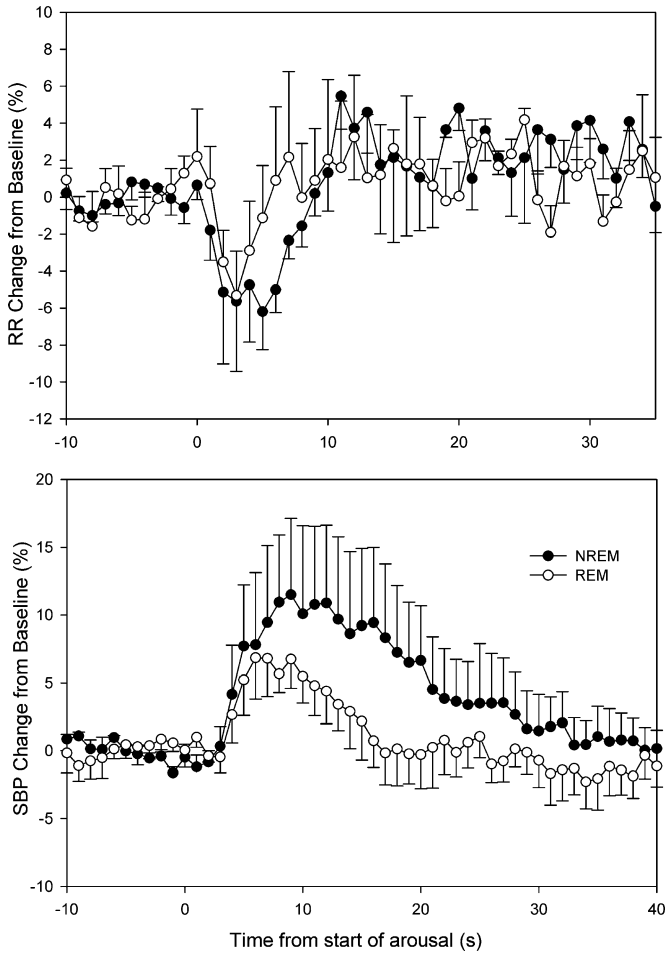

Fig. 4. Group-averaged (± standard errors) changes in R-R interval and systolic blood pressure following arousal from NREM (filled circles) and REM (open circles) sleep. Time t = 0 represents the start of the arousal.

of the variance performed with post-stimulus time being the single factor. All time courses were represented in terms of % of change from the average baseline level (computed as the pre-stimulus average). Thus, the objective of the statistical analysis was to ascertain whether there was "significant change" in the time-course of each parameter post-arousal versus pre-arousal. Post-hoc Dunn's pairwise comparisons identified the points in time where the discrepancies versus baseline occurred. Comparisons between sleep stages were performed using two-way repeated-measures analysis of variance, with *stage* being one factor and *time* the other factor. Thus, interaction (*stage X time*) was used to identify time-course differences in arousal responses between stages. Post-hoc Tukey tests were used to locate where the averaged time courses between sleep stages differed. A p-value <0.05 was considered to be significant.

III. Results

A. Cardiovascular Changes Following Arousal

The subject-averaged changes in RRI and SBP from their pre-arousal baselines are displayed in Fig. 4, with filled circles representing NREM sleep and open circles representing REM sleep. In both NREM and REM sleep, there were rapid reductions in RRI (or equivalently, increases in heart rate) which lasted for only about 10 s post-arousal. There was a brief latency of 2–3 s before the arousal-induced increases in SBP were observed; these SBP increases persisted for between 20–30 s post-arousal. In both NREM and REM sleep, the increases in SBP were highly significant ($P < 0.005$). Although the average magnitude of the increase in SBP was larger in NREM sleep relative to REM sleep (Fig. 4, bottom panel), there was no statistical difference between the time-courses representing the two sleep stages.

B. Impulse Response Behavior During Arousal

Table I summarizes the results of the statistical analysis performed on the time-courses of the impulse response descriptors. The one-way repeated-measures ANOVA (RMANOVA) time effect (shown for arousal from NREM and REM sleep stages in columns 3 and 4, respectively) provides an indication of whether or not the time courses were affected by arousal. The two-way RMANOVA *time X stage* effect (column 5) indicates whether the arousal-induced changes occurring in the two stages of sleep have different time courses. The impulse response magnitudes for all 4 model components were significantly affected by arousal during NREM sleep, except for the RSA component

TABLE I
RESULTS OF THE STATISTICAL ANALYSIS FOR THE AROUSAL RESPONSES IN THE IMPULSE RESPONSE COMPACT DESCRIPTORS IN NREM AND REM SLEEP. COLUMNS 3 AND 4 DISPLAY THE P-VALUES FOR SIGNIFICANCE IN TIME EFFECT OBTAINED FROM ONE-WAY RMANOVA; COLUMN 5 SHOWS THE P-VALUE FOR TIME X SLEEP-STAGE INTERACTION USING TWO-WAY RMANOVA

IR	IR Descriptors	NREM	REM	*NREM vs. REM*
	Magnitude	<0.001	NS	*0.017*
RSA	Dynamic Gain	NS	NS	*NS*
	Characteristic Time	0.023	0.007	*NS*
	Magnitude	< 0.001	< 0.001	*NS*
ABR	Dynamic Gain	< 0.001	0.004	*0.031*
	Characteristic Time	< 0.001	NS	*NS*
	Magnitude	0.002	0.001	*NS*
CID	Dynamic Gain	NS	< 0.001	*NS*
	Characteristic Time	NS	0.049	*NS*
	Magnitude	0.028	0.043	*NS*
DER	Dynamic Gain	NS	<0.001	*< 0.001*
	Characteristic Time	*0.007*	*NS*	*NS*

during REM sleep. The corresponding results for dynamic gain and characteristic time appeared less sensitive in detecting the arousal-induced changes.

C. Impulse Response Descriptors During NREM Arousals

The magnitude of the RSA impulse responses demonstrated an increase that lasted up to 30 s post-arousal (Fig. 5, top left panel). Post-hoc pair wise comparisons with Dunn's test showed that the RSA impulse response magnitude was significantly altered from baseline for up to ∼20 s following the arousal stimulus. On the other hand, the estimated time-courses for dynamic gain were more variable and did not reflect the abrupt changes so faithfully. The estimated profile of characteristic time of the RSA impulse response showed a rapid decrease during NREM arousal, suggesting a more rapid response of heart rate to changes in respiration immediately after arousal. This downward tendency starts almost immediately after the stimulus, and lasts for ∼18 s.

The baroreflex (ABR) response to arousal consisted of a rapid increase in magnitude immediately after arousal for up to 10 s post-stimulus (Fig. 5, top right panel) with a subsequent undershoot from ∼15 s to 30 s following the start of arousal. This tendency to oscillate was noticeable in the time-courses of the dynamic gain descriptor as well. Statistical analysis confirmed that these changes in impulse response magnitude and dynamic gain were significant $(\mathrm{P} < 0.05)$. There was also an increase in ABR characteristic time during the first 20 s post-arousal $(\mathrm{P} < 0.001)$, followed by a smaller subsequent undershoot.

There was a significant increase in CID magnitude following arousal (Fig. 5, bottom left panel). This increase appeared to last for ∼10 s post-arousal, but there was considerable variability across subjects. The DER impulse response magnitude also displayed a significant increase following arousal (Fig. 5, bottom right panel).

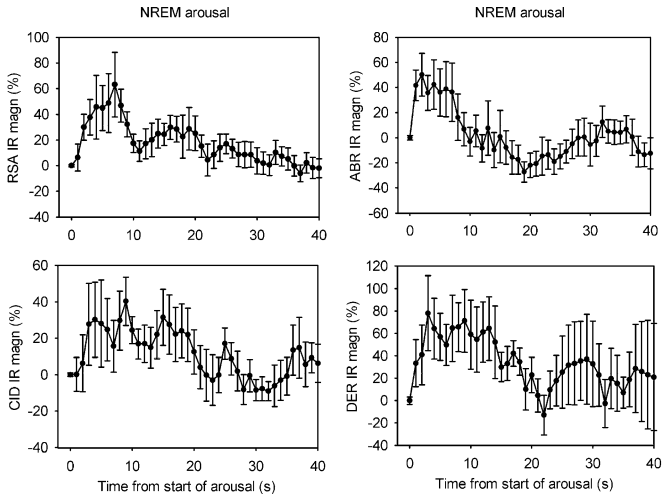

Fig. 5. Time-courses of the estimated impulse response magnitudes for the RSA (top left panel), ABR (top right panel), CID (bottom left panel) and DER (bottom right panel) in NREM arousal.

D. NREM versus REM Arousal

In REM sleep, arousal did not produce changes in the magnitude of the RSA component. Fig. 6 (top left panel) compares the average RSA impulse response magnitude time-course in REM sleep (open circles) with the corresponding time-course in

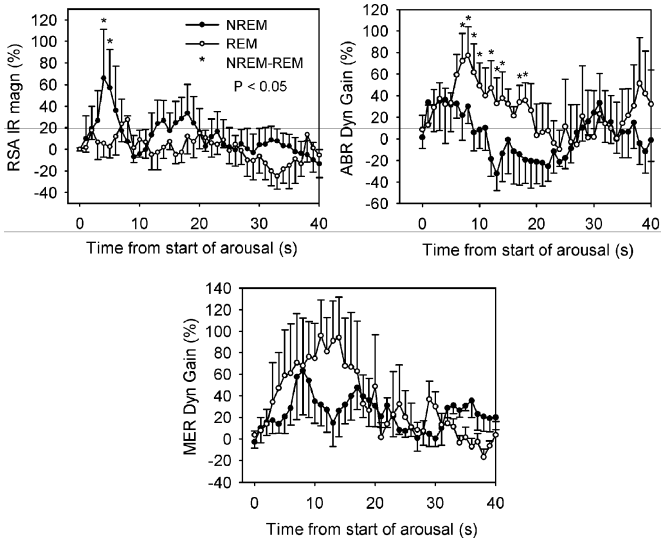

Fig. 6. Comparisons between NREM (filled circles) and REM (open circles) sleep in the RSA impulse response magnitude (top left panel), ABR dynamic gain (top right panel), and DER dynamic gain (bottom panel).

NREM sleep (closed circles). The largest differences occurred during the first 8 s post-arousal.

Unlike RSA, the ABR gain descriptors showed significant changes during REM arousal. These changes paralleled those occurring during NREM arousal, but tended to be larger in magnitude. The time-course for ABR dynamic gain showed a significantly larger increase post-arousal in REM vs NREM (Fig. 6, top right panel). ABR characteristic time did not change during arousal from REM sleep.

The effect of REM arousal on the CID impulse response descriptors was largely similar to the effect of NREM arousal. Arousal produced a larger impact on the DER gain descriptors in REM sleep versus NREM sleep; however, only the time-course in DER dynamic gain showed differences between the two stages of sleep (Fig. 6, bottom panel).

IV. Discussion

In the present study, we have employed a closed-loop model analysis to determine the responses of the cardiovascular control system to transient arousals from NREM and REM sleep. The model is useful in allowing us to characterize the dynamics of the functional mechanisms that mediate the interactions among respiration, heart rate and blood pressure, as well as to impose causality constraints on the model structure in order to computationally partition the feedforward from the feedback components of the model. Recent studies have established that sympathetic tone is markedly elevated in subjects with OSAS and that this autonomic abnormality is likely to play a major role in placing them at increased risk for cardiovascular disease [1], [2]. The alteration in autonomic function is believed to result from chronic exposure to the repetitive episodes of hypoxia and arousal from sleep associated with upper airway obstruction. The question that we have begun to explore in this study is whether intermittent sympathetic activation produced by periodic arousal alone can lead to chronic elevations of blood pressure, and if so, what mechanisms might mediate this long-term effect.

A strength of the method of analysis employed in this work is the use of the Laguerre expansion technique which permitted a drastic reduction of model parameters, making the model formulation more amenable for extension to the time-varying case. By applying the recursive least squares algorithm on the expansion coefficients instead of all samples of the impulse response function, we were able to obtain more robust time-varying parameter estimate and also reduce the memory length λ of the algorithm. This, in turn, improved the speed of response of the algorithm in tracking dynamic changes in the model properties. Nevertheless, as tests with simulated data indicated, the algorithm is limited in time-resolution by the finite adaptation time of between 10–20 s. Since a significant portion of the post-arousal cardiorespiratory response occurs within 20 s, it is important to bear in mind that the algorithm likely **underestimates** the magnitude of the changes in the component impulse responses in the early part of the response.

A. Mechanisms Modulating RRI Variability: RSA and ABR Responses to Arousal

The consensus among sleep physiologists is that the immediate response in heart rate to arousal represents a parasympathetic withdrawal. However, in our previous study [9], we showed that this rapid increase in heart rate is strongly associated with a concomitant increase in ventilation during arousal. In the present study, we found that in REM sleep, this increase in heart rate was larger than it would be expected if the respiratory-cardiac coupling gain were to remain unchanged by arousal. To account for the additional increase in heart rate, it was inevitable for the model to predict that the gain of the coupling between respiration and heart rate (RSA gain) increased during arousal. Thus, although arousal was associated with a large and rapid parasympathetic withdrawal, the gain of the modulation of parasympathetic activity actually increased. It appears likely that the increase in RSA gain was a secondary effect of the enhanced ventilatory response to arousal, since it has been shown that RSA gain increases with increases in tidal volume [19]. However, during REM sleep, it appears that this increase in RSA gain is blunted, in spite of the fact that the ventilatory responses to arousal during NREM and REM sleep are not different. We speculate that this difference in REM sleep may be related to the predominance of the sympathetic nervous system during that state [20].

A previous study has shown that hyperventilation actually blunts the sensitivity of the baroreflex [21]. Thus, it appears unlikely that the rapid increase in baroreflex gain that occurred in the first 10 s post-arousal was associated with the concomitant increase in ventilation. Although it is unclear what mechanism was responsible for the transient increase in baroreflex gain, the transient elevation of baroreflex gain was probably useful in buffering the large increase in heart rate produced by arousal. As well, the increase in baroreflex gain probably played an important role in delaying the post-arousal increase in SBP.

A somewhat surprising finding is that the arousal-induced initial increase in baroreflex gain was larger in REM than NREM sleep. However, a recent study by Legramante *et al.* [22] found that the baroreflex sensitivity in response to hypertensive stimuli during REM sleep is higher than baroreflex sensitivity during NREM sleep and wakefulness. This may reflect a compensatory

response by the body to buffer the increased sympathetic activation that accompanies REM sleep. After the initial 10 s post-arousal, our findings show that baroreflex gain tends to remain below baseline for some time. This subsequent depression in baroreflex gain could be the main factor responsible for the relatively long-lasting post-arousal elevation of sympathetic tone that we had reported previously [9].

B. Mechanisms Modulating SBP Variability: CID and DER Responses to Arousal

The CID impulse response magnitude increased in the post-arousal period, but this increase started to occur only after the first few seconds following the start of arousal. This delay in the CID arousal response suggests that the transient increase in CID results from peripheral vasoconstriction (and hence, increased vascular resistance), which assumes a slower time-course than sympathetically-induced changes in the heart. In combination with an increase in cardiac output, the elevated vascular resistance results in a larger increase of SBP. Peripheral vasoconstriction probably accounts for the increased CID gain for up to $\sim$20 s after the arousal. These findings are consistent with those of O'Leary and Woodbury [23], who demonstrated that LF oscillations of blood pressure are due more to changes in peripheral resistance than changes in cardiac output.

The transient increase in DER gain during both NREM and REM arousals was also a surprising finding. A previous study by our group [24] showed that upper airway resistance decreases almost immediately following the start of an arousal. A reduction in upper airway resistance would produce smaller fluctuations in blood pressure for a given ventilatory effort and, thus, should have led to a reduction in DER gain. It is unlikely that intrathoracic mechanics could have changed so rapidly and transiently. These considerations suggest that the increase in DER gain was probably related to a sympathetically-mediated elevation in heart contractility, which amplified respiratory-synchronous fluctuations in stroke volume [15].

C. Limitations of the Study

An important limitation of this work relates to our definition of "arousals" as EEG accelerations lasting 3 s or longer. Although this conforms to the standard advocated by the American Academy of Sleep Medicine (AASM) [5], some reports have pointed out an association between the association between transient state changes and K-complexes and delta bursts, which may also have a cardiovascular impact [25]. Events that did not satisfy the 3-second criteria accounted for only a small percentage of all experiments performed on the subjects, since the acoustic stimulation was continually adjusted to maximize the occurrences of AASM arousals. Furthermore, in a previous study [9], when we compared arousal with "nonarousal" trials, there was significantly less cardiovascular activity triggered by the "nonarousals" versus the AASM arousals.

Another limitation of our work concerns the patterns of different physiological behavior observed in NREM Stage 2 sleep. It has been reported that Stage 2 consists of both stable periods as well as periods with considerable phasic activation. In our analyses, we did not discriminate between these different modes of Stage 2 behavior. As well, in our study, we did not discriminate between the cardiovascular effects of arousal during tonic versus phasic REM sleep. The conditions of our experiments were not conducive to the occurrence of REM, and thus, the number of data segments in REM that were available for analysis was relatively small. These unresolved issues warrant further exploration in future studies.

V. Conclusion

In this paper, we employed a time-varying closed-loop model to gain better insight into and to quantitatively characterize the major physiological mechanisms underlying cardiorespiratory variability during arousal from sleep. Time-domain system identification techniques were used to partition feedback from feedforward influences in this closed-loop system, enabling the time-varying impulse responses of the model components to be estimated. By applying a combination of the recursive least-squares algorithm (RLS) and the Laguerre expansion of kernels technique, we were able to reduce the parametrization of the problem and, thus, obtain robust parameter estimates.

We found that during transient arousal from sleep: 1) RSA gain increases in NREM but not in REM sleep; 2) ABR gain shows an initial increase (more pronounced in REM versus NREM sleep), followed by a more sustained decrease below pre-arousal baseline levels, which allows sympathetic tone to remain elevated for $>$30 s post-arousal; 3) an increase in CID gain with arousal that is consistent with increased systemic vascular resistance; 4) a transient increase in DER gain, which may reflect increased sympathetic modulation of cardiac contractility, during both NREM and REM arousals. These findings establish a normative database against which further measurements of cardiovascular arousal responses in OSAS may be compared. In particular, alterations in the cardiovascular response to arousal may provide a useful index of the severity of autonomic dysfunction in OSAS, similar to the impaired peripheral vasodilatory responses to hypoxia that have been reported in these subjects [27].

Appendix
Method for Estimating the Model Impulse Responses

The Laguerre expansion of kernels technique [16] was used in this study since others have demonstrated that it is well suited for estimating the linear and nonlinear system kernels from input-output signals [16], and that it works well even when only short data series are available. In this work, we have found that it does not require as much adaptation time as other methods such as those assuming autoregressive models with exogenous input. This allows shorter data sets to be studied. The reduction in parametrization is significant with this method, which enhances the robustness of the parameter estimates.

A. Time-Varying Laguerre Expansion Technique Applied to the Model

In this paper, nonlinearities were ignored, but the linear system kernels (impulse responses) were allowed to be time-varying. For a system with two inputs x and u, the output y at time t was expressed as the sum of the resulting functions

obtained when each input was convolved with its corresponding kernel as follows:

$$y(t) = \sum_{\tau=0}^{N-1} h_x(\tau,t)\cdot x(t-\tau-D_x) + \sum_{\tau=0}^{N-1} h_u(\tau,t)\cdot u(t-\tau-D_u) + \varepsilon(t) \quad (4)$$

where N is the duration of the kernels, and D_x, D_u are the delays between each input and the output. $\varepsilon(t)$ is the residual error resulting from the estimation of the model. The impulse responses, h_x and h_u, were expressed as Laguerre expansions in the following way:

$$h_x(\tau,t) = \sum_{k=0}^{P-1} a_k(t)\cdot L_k(\tau)$$
$$h_u(\tau,t) = \sum_{k=0}^{Q-1} b_k(t)\cdot L_k(\tau) \quad (5)$$

where P and Q are the number of Laguerre functions required to characterize each kernel and L_k is the Laguerre function of order k, and $a_k(t)$ and $b_k(t)$ are the time-varying expansion coefficients. By inserting (4) in (3) and rewriting, we obtain

$$y(t) = \sum_{\tau=0}^{P-1}\sum_{k=0}^{N} a_k(t)\cdot L_k(\tau)\cdot x(t-\tau-D_x) + \sum_{\tau=0}^{Q-1}\sum_{k=0}^{N} b_k(t)\cdot L_k(\tau)\cdot u(t-\tau-D_u) + \varepsilon(t). \quad (6)$$

To obtain a more compact expression, the convolution of each input and the corresponding Laguerre functions can be rewritten as

$$v_k(t) = \sum_{\tau=0}^{P-1} L_k(\tau)\cdot x(t-\tau-D_x)$$
$$w_k(t) = \sum_{\tau=0}^{Q-1} L_k(\tau)\cdot u(t-\tau-D_u). \quad (7)$$

Then

$$y(t) = \sum_{k=0}^{N} a_k(t)\cdot v_k(t) + \sum_{k=0}^{N} b_k(t)\cdot w_k(t) + \varepsilon(t) \quad (8)$$

which can be solved using the RLS algorithm.

B. Model Order Determination and Parameter Estimation

It was necessary to first determine the number of Laguerre functions required to adequately characterize the impulse responses, the delays corresponding to each of the model components, and the decay rate of the Laguerre functions characterized by the parameter α. For a specific value of α, the following criteria were applied to determine the optimal combination of the number of Laguerre functions and component delays.

- Minimum description length (MDL), with var(ξ) being the variance of the residuals, N the total length of the signals and K the number of Laguerre functions

$$\mathrm{MDL} = \log(\mathrm{var}(\xi)) + \log(N)\cdot\frac{K}{(2N)}. \quad (9)$$

- Lack of significant correlation between the residuals and each of the inputs.

Once the number of Laguerre functions and the component delays were set, the parameter α was chosen so that the expansion functions decayed to zero prior to the maximum expected duration of the impulse response [16]. This process was repeated for the entire range of combinations of parameters, and the optimal structure was selected based on the model that produced the global minimum value of MDL.

Subsequently, the selected model structure was kept fixed, while the recursive least squares algorithm was implemented to estimate the model coefficients in an adaptive manner from the entire data sequence. This was repeated for a range of λ values. For each λ value, the normalized mean-square error between the measured output and the model prediction was calculated. The λ value that produced the minimum normalized mean-square error was selected to be the optimal memory length for that dataset. The average value of λ was 0.898.

REFERENCES

[1] R. S. T. Leung and T. D. Bradley, "Sleep apnea and cardiovascular disease," *Am. J. Respir. Crit. Care Med.*, vol. 164, pp. 2147–2165, 2001.

[2] V. K. Somers, M. E. Dyken, M. P. Clary, and F. M. Abboud, "Sympathetic neural mechanisms in obstructive sleep apnea," *J. Clin. Invest.*, vol. 96, pp. 1897–1904, 1995.

[3] A. Xie, J. B. Skatrud, D. S. Puleo, and B. J. Morgan, "Exposure to hypoxia produces long-lasting sympathetic activation in humans," *J. Appl. Physiol.*, vol. 91, pp. 1555–1562, 2001.

[4] D. Brooks, R. L. Horner, L. F. Kozar, C. L. Render-Teixeira, and E. A. Phillipson, "Obstructive sleep apnea as a cause of systemic hypertension: evidence from a canine model," *J. Clin. Invest.*, vol. 99, pp. 106–109, 1997.

[5] Sleep Disorders Atlas Task Force of the ADERican Sleep Disorders Association, EEG arousals: scoring rules and examples, in Sleep, vol. 15, pp. 173–184, 1992.

[6] P. D. Catcheside, S. C. Chiong, R. S. Orr, J. DERcer, N. A. Saunders, and R. D. McEvoy, "Acute cardiovascular responses to arousal from non-REM sleep during normoxia and hypoxia," *Sleep*, vol. 24, pp. 895–902, 2001.

[7] R. J. O. Davies, P. J. Belt, S. J. Roberts, N. J. Ali, and J. R. Stradling, "Arterial blood pressure response to graded transient arousal from sleep in normal humans," *J. Appl. Physiol.*, vol. 74, pp. 1123–1130, 1993.

[8] B. J. Morgan, D. C. Crabtree, D. S. Puleo, M. S. Badr, F. Toiber, and J. B. Skatrud, "Neurocirculatory consequences of abrupt change in sleep state in humans," *J. Appl. Physiol.*, vol. 80, pp. 1627–1636, 1996.

[9] A. Blasi, J. Jo, E. Valladares, B. J. Morgan, J. B. Skatrud, and M. C. K. Khoo, "Cardiovascular variability after arousal from sleep: time varying spectral analysis," *J. Appl. Physiol.*, vol. 95, pp. 1394–1404, 2003.

[10] R. D. Berger, S. Askelrod, D. Gordon, and R. J. Cohen, "An efficient algorithm for spectral analysis of heart rate variability," *IEEE Trans Biomed Eng*, vol. BME-33, pp. 900–904, 1986.

[11] V. Belozeroff, R. B. Berry, C. S. H. Sasson, and M. C. K. Khoo, "Effects of CPAP therapy on cardiovascular variability in obstructive sleep apnea: a closed-loop analysis," *Am. J. Physiol. (Heart Circ. Physiol.)*, vol. 282, pp. H110–H121, 2002.

[12] J. Jo, A. Blasi, E. Valladares, R. Juarez, A. Baydur, and M. C. K. Khoo, "Model-based assessment of autonomic control in obstructive sleep apnea syndrome during sleep," *Am. J. Resp. Crit. Care Med.*, vol. 167, pp. 128–136, 2003.

[13] G. Baselli, S. Cerutti, S. Civardi, A. Malliani, and M. Pagani, "Cardiovascular variability signals: toward the identification of a closed-loop model of the neural control mechanisms," *IEEE Trans. Biomed. Eng.*, vol. 35, no. 12, pp. 1033–1045, Dec. 1988.

[14] T. J. Mullen, M. L. Appel, R. Mukkamala, J. M. Mathias, and R. L. Cohen, "System identification of closed-loop cardiovascular control: effects of posture and autonomic blockade," *Am. J. Physiol.*, vol. 272, pp. H448–H461, 1997.

[15] K. Toska and M. Eriksen, "Respiration-synchronous fluctuations in stroke volume, heart rate and arterial pressure in humans," *J. Physiol.*, vol. 472, pp. 501–512, 1993.

[16] V. Z. Marmarelis, "Identification of nonlinear biological systems using Laguerre expansions of kernels," *Ann. Biomed. Eng.*, vol. 21, pp. 573–589, 1993.

[17] S. Haykin, "Linear prediction," in *Adaptive Filter Theory*, 3rd ed. Upper Saddle River, NJ: Prentice-Hall, 1996, pp. 562–588.

[18] M. C. K. Khoo, "Time-domain analysis of linear control systems," in *Physiological Control Systems. Analysis, Simulation and Estimation*. ser. Biomedical Engineering, M. Akay, Ed. Piscataway, NJ: IEEE Press, 1999, pp. 69–99.
[19] T. E. Brown, L. A. Beightol, J. Koh, and D. L. Eckberg, "Important influence of respiration on human R-R interval power spectra is largely ignored," *J. Appl. Physiol.*, vol. 75, pp. 2310–2317, 1993.
[20] G. Mancia, "Autonomic modulation of the cardiovascular system during sleep," *N. Engl. J. Med.*, vol. 328, pp. 347–349, 1993.
[21] P. Van de Borne, S. Mezzetti, N. Montano, K. Narkiewicz, J. P. Degaute, and V. K. Somers, "Hyperventilation alters arterial baroreflex control of heart rate and muscle sympathetic nerve activity," *Am. J. Physiol.*, vol. 279, pp. H536–H541, 2000.
[22] J. M. Legramante, M. G. Marciani, F. Placidi, S. Aquilani, A. Romigi, M. Tombini, M. Massaro, A. Galante, and F. Iellamo, "Sleep-related changes in baroreflex sensitivity and cardiovascular autonomic modulation," *J. Hypertens.*, vol. 21, pp. 1555–1561, 2003.
[23] D. S. O'Leary and D. J. Woodbury, "Role of cardiac output in mediating arterial blood pressure oscillations," *Am. J. Physiol.*, vol. 271, pp. R641–R646, 1996.
[24] M. C. K. Khoo, S. S. W. Koh, J. J. W. Shin, P. R. Westbrook, and R. B. Berry, "Ventilatory dynamics during transient arousal from NREM sleep: implications for respiratory control stability," *J. Appl. Physiol.*, vol. 80, pp. 1475–1484, 1996.
[25] J. Tank, A. Diedrich, N. Hale, F. E. Niaz, R. Furlan, R. M. Robertson, and R. Mosqueda-Garcia, "Relationship between blood pressure, sleep K-complexes, and muscle sympathetic nerve activity in humans," *Am. J. Physiol. Regul. Integr. Comp. Physiol.*, vol. 285, pp. R208–R214, 2003.
[26] F. Iellamo, F. Placidi, M. G. Marciani, A. Romigi, M. Tombini, S. Aquilani, M. Massaro, A. Galante, and J. M. Legramante, "Baroreflex bufferning of sympathetic activation during sleep. Evidence from autonomic assessment of sleep macroarchitecture and microarchitecture," *Hypertension*, vol. 43, pp. 814–819, 2004.
[27] Remsburg, S. H. Launois, and J. W. Weiss, "Patients with obstructive sleep apnea have an abnormal peripheral vascular response to hypoxia," *J. Appl. Physiol.*, vol. 87, pp. 1153–1158, 1999.

Anna Blasi received the B.S. degree in industrial engineering from the Politecnic University of Catalunya (UPC), Barcelona, Spain, in 1997. While working on the final project of the B.S. degree she did some research at the Centre de Recerca en Enginyeria Biomedica (CREB) from UPC. She received the M.S. degree in biomedical engineering in the same research center in 1997. She received the Ph.D. degree in biomedical engineering from the University of Southern California, Los Angeles, in 2004. Her Ph.D. research involved the study of the effects of Obstructive Sleep Apnea on the cardiovascular control.

Her research interests have revolved mainly around the cardiovascular system, starting with the work she conducted at the CREB, where she worked on the detection of heart rate anomalies. Other research topics of her interest are related with cerebral function. While in Barcelona, for her M.S. thesis she worked at the Escola de Patologia del Llenguatge (Language Pathologies unit of the Hospital de la Santa Creu i Sant Pau), developing a software for the rehabilitation of aphasia patients. She is currently with the Department of Medical Physics and Bioengineering, University College London, London, U.K., where she holds a Postdoctoral Fellowship to study the development of cerebral function in babies.

Javier Antonio Jo received the Diploma in electrical engineering from the Pontifical Catholic University of Peru, Lima, Peru, in 1997, the M.S. degree in electrical engineering and the Ph.D. degree in biomedical engineering from the University of Southern California, Los Angeles, in 2000 and 2002, respectively. He is currently a Research Scientist at the Department of Surgery of Cedars-Sinai Medical Center, Los Angeles, CA.

His research interests include biomedical signal processing and modeling of nonlinear and time-varying systems. He is particularly interested in physiological modeling of cardiovascular autonomic and respiratory control during sleep, and developing of advanced analytical methods for time-resolved fluorescence spectroscopy and imaging with application in cardiovascular and cancer diagnosis.

Dr. Jo is a member of the Biomedical Engineering Society (BMES), the IEEE Engineering in Medicine and Biology Society, the IEEE Signal Processing Society, the International Society of Optical Engineering (SPIE), the American Society for Lasers in Medicine and Surgery (ASLMS), and The National Honor Society of Phi Kappa Phi.

Edwin Valladares received the B.S. degree in biomedical engineering from the University of Southern California (USC), Los Angeles, in 1999.

From 1997 to 2002, he was a Research Associate and subsequently a Project Manager at the Cardiorespiratory Laboratory at USC. Since January 2002, he has been Director of the Sleep Laboratory at the University of California at Los Angeles Cousins Center for Psychoneuroimmunology, The Neuropsychiatric Institute, Los Angeles, CA. His current interests include autonomic regulation and interactions between sleep and the immune system within substance abuse populations, mainly alcohol and cocaine.

Mr. Valladares became a registered polysomnography technologist (RPsgT) in 1999. He is a member of the American Academy of Sleep Medicine and the American Heart Association.

Ricardo Juarez is Assistant Professor of Medicine and Medical Director of the Sleep Diagnostics Program at the University of Southern California, Los Angeles.

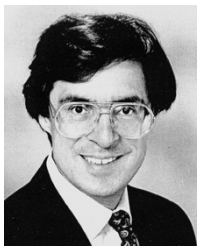

Ahmet Baydur graduated from Wayne State University School of Medicine, Detroit, MI, in 1970.

He completed a medical internship and residency in 1973, and a pulmonary fellowship at Los Angeles County and the University of Southern California (USC) in 1975, and at Rancho Los Amigos National Rehabilitation Center (RLANRC), Downey, CA, in 1976. He also completed a respiratory physiology fellowship at the Meakins-Christie Laboratories, McGill University, Montreal, QC, Canada in 1980. He has been on the faculty of the Keck School of Medicine, USC since 1977, and is currently Professor of Clinical Medicine in the Division of Pulmonary and Critical Care Medicine. He was also on the staff at RLANRC for 20 years (six years as Director of the Chest Medicine Service) before returning to the Keck School of Medicine Health Sciences Campus in 1996. His interests include respiratory mechanics, control of ventilation, neuromuscular and chest wall disorders, and noninvasive ventilation

Michael C. K. Khoo (M'86) received the B.Sc.(Eng.) degree in mechanical engineering from Imperial College of Science and Technology, University of London, in 1976, and the M.S. and Ph.D. degrees in bioengineering from Harvard University, Cambridge, MA, in 1977 and 1981, respectively.

From 1981 to 1983, he was a Research Associate at the V.A. Hospital, West Roxbury, MA, and the Brigham and Women's Hospital, Boston, MA. Since September 1983, he has been on the faculty of the University of Southern California, Los Angeles, where he is currently Professor and Chairman of Biomedical Engineering. He is also Co-Director of Education and Outreach in the Biomimetic Microelectronic Systems Engineering Research Center at USC. His current research interests include cardiorespiratory regulation and variability in sleep apnea, physiological modeling, and biomedical signal processing.

Dr. Khoo is a Fellow of the American Institute of Medical and Biological Engineering and the Biomedical Engineering Society, as well as a member of the American Physiological Society, American Academy of Sleep Medicine, and the American Heart Association. He is also on the editorial board of the IEEE Press Book Series on Biomedical Engineering. He is the author of the biomedical engineering textbook: *Physiological Control Systems: Analysis, Simulation and Estimation* (Wiley-IEEE Press, 2000).